Humidity sensing by nanocomposites of silver in silicate glass ceramics

B. N. Pal, T. K. Kundu, S. Banerjee, and D. Chakravorty

Citation: Journal of Applied Physics **93**, 4201 (2003); doi: 10.1063/1.1559427
View online: http://dx.doi.org/10.1063/1.1559427
View Table of Contents: http://scitation.aip.org/content/aip/journal/jap/93/7?ver=pdfcov
Published by the AIP Publishing

Humidity sensing by nanocomposites of silver in silicate glass ceramics

B. N. Pal
Indian Association for the Cultivation of Science, Kolkata-700 032, India

T. K. Kundu
Department of Physics and Technophysics, Vidyasagar University, Midnapore-721 102, India

S. Banerjee
Department of Physics, University of Calcutta, Kolkata-700 009, India

D. Chakravorty[a)]
Indian Association for the Cultivation of Science, Kolkata-700 032, India

(Received 9 October 2002; accepted 15 January 2003)

Silver nanoparticles of diameters in the range 3.4 to 13.2 nm were grown within a silicate glass ceramics containing barium titanate phase. The glass ceramics were filled with silver particles by subjecting the former to a $Na^+ - Ag^+$ ion exchange process followed by a reduction treatment in hydrogen. Silver particles were formed at the interfaces of the silicate glass and the barium titanate phases, respectively. The silver particle sizes could be varied by controlling the fractal structure of the crystalline phase by prior heat treatment. Electrical resistivity measurements were carried out on cold-pressed specimens of nanocomposite powders prepared as just stated. A five order of magnitude resistivity change was recorded in the case of nanocomposite specimen with a silver particle diameter of 10.1 nm in the relative humidity range of 25% to 85%. The resistivity of the nanocomposites was found to be controlled by a variable range hopping conduction. It is believed that the silver nanoparticles provide sites where physisorption of water molecules takes place which increases the number of localized states near the Fermi level. © *2003 American Institute of Physics.* [DOI: 10.1063/1.1559427]

I. INTRODUCTION

Humidity sensors have assumed importance in recent years because of the need to monitor and control environmental humidity in various industrial processes.[1] For automated control of humidity, sensors using changes of electrical conductivity are necessary. Research has been carried out on various systems to explore the possibility of utilizing them as humidity sensors.[2–8] Commercial humidity sensors are mostly comprised of either polymer films[9,10] or porous ceramics.[11,12] These sensors are based on the principle of electrical resistance change as a function of relative humidity. Adsorption of water molecules on the surface of these systems causes their electrical properties to change. Essentially, two types of sensors have been reported. In the ionic-type sensors, protons are the charge carriers which hop between adjacent hydroxyl groups on application of electric field.[13] In the electronic-type humidity sensors, water molecules are chemisorbed on semiconducting oxides and electrons are injected to the latter from the former thereby changing the resistivity of the semiconductor.[14] Nanocomposites are characterized by the dispersion of nanosized metals or semiconductors within an inert matrix.[15] Some of the examples are silver, copper, nickel, or lead sulphide within a silicate glass.[16,17] The dispersoids have a large surface-to-volume ratio. This makes these materials potentially attractive for sensing purposes because, in principle, they should provide innumerable surface sites for physisorption of water molecules. We have explored such possibilities in nanocomposites containing silver particles grown within a glass–barium titanate composite by the ion exchange followed by reduction technique.[18] Large changes in resistivity were observed as a function of relative humidity. Also, the electrical resistivity was found to be electronic in nature. The details are reported in this article.

II. EXPERIMENT

The glass composition used in this investigation was $10\,Na_2O \cdot 34\,BaO \cdot 34\,TiO_2 \cdot 17\,B_2O_3 \cdot 5\,SiO_2$ (in mol %). The crystalline phase grown within this glass was $BaTiO_3$. We had earlier worked on this system because of unusual dielectric properties exhibited by the specimens.[19] For preparing the glass, the raw materials used were reagent grade chemicals Na_2CO_3, $BaCO_3$, TiO_2, H_3BO_3, and SiO_2, respectively. A mixture of required amounts of these chemicals was taken in an alumina crucible. The glass was melted in an electrically heated furnace at a temperature of 1400 K. Glass was cast by pouring the melt onto an aluminum mold.

The nucleation and growth temperatures for the crystalline phase $BaTiO_3$ were determined by differential thermal analysis (DTA) carried out on the glass sample using a Shimadzu DT40 apparatus. The endo- and exothermic peaks in the DTA curve corresponded to the nucleation and growth temperatures, respectively.[18] The crystalline phases grown within the glass after the heat treatment were identified from the powder diffraction pattern taken in a Rich Seifert 3000P x-ray diffractometer using Cu $K\alpha$ radiation.

[a)]Electronic mail: mlsdc@mahendra.iacs.res.in

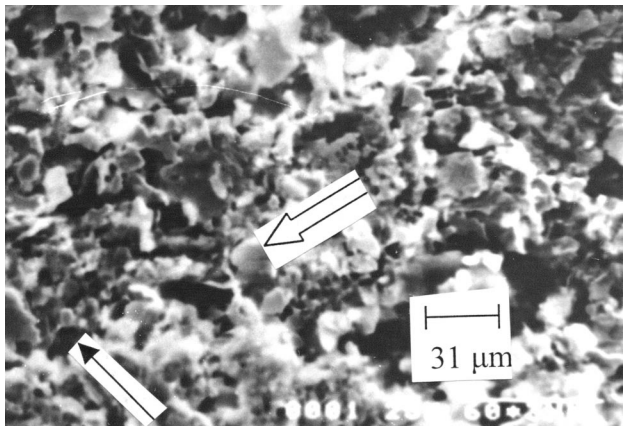

FIG. 1. Scanning electron micrograph of glass heat treated at 843 K for 6 h followed by 963 K for 15 min.

Glass–ceramic samples were made by giving different heat treatments to the glass. Essentially, the durations of treatment at the nucleation and growth temperatures, respectively, were varied. It has been shown earlier that the fractal structure of the crystalline phase can be varied by such treatments.[20] Such a variation of the morphology of the crystalline phase changes the growth rate of the metallic phase. The nanometer-sized metal can be grown at the interface of the crystal and the glass after the ion-exchanged (with silver ions) glass ceramic is subjected to a reduction treatment in hydrogen.[16] The metal particle diameter can be changed by growing them in glass ceramics having different fractal dimensions of the crystalline phase without altering the reduction temperature and time. This has been discussed in detail elsewhere.[20] In the present investigation, the glass–ceramic samples were, first, ground using a mortar and pestle so that the particle sizes were ~5 μm. The sodium/silver ion exchange was carried out by immersing the powder in a molten bath of silver nitrate kept in a pyrex boat at a temperature of 583 K for a period of 6 h. After the interdiffusion reaction, the samples were washed in distilled water to remove any silver nitrate adhering to the sample surfaces. All of the ion-exchanged specimens were reduced in a stream of hydrogen at a temperature of 573 K for 5 min.

The microstructure of the glass–ceramic samples was studied by a scanning electron microscope (Hitachi model No. S-415A). The microstructure of the ion-exchanged and reduced glass–ceramic samples was investigated using a JEM 200 CX transmission electron microscope (TEM). The details of specimen preparation for TEM studies were described earlier.[21]

For electrical measurements under different RH conditions, specimens with an area of 0.5 cm^2 and thickness 0.3 cm were prepared by pressing the powders prepared as just stated with a load of 10 tons. Silver paint electrodes (supplied by Acheson Colloiden B.V. Holland) were applied to the two opposite faces of the cold-pressed specimens. The specimens were mounted in a glass chamber with provision of a stopcock so that it could be evacuated or filled with gases if required. To generate a different RH, the chamber was partially evacuated by a mechanical pump, the stopcock

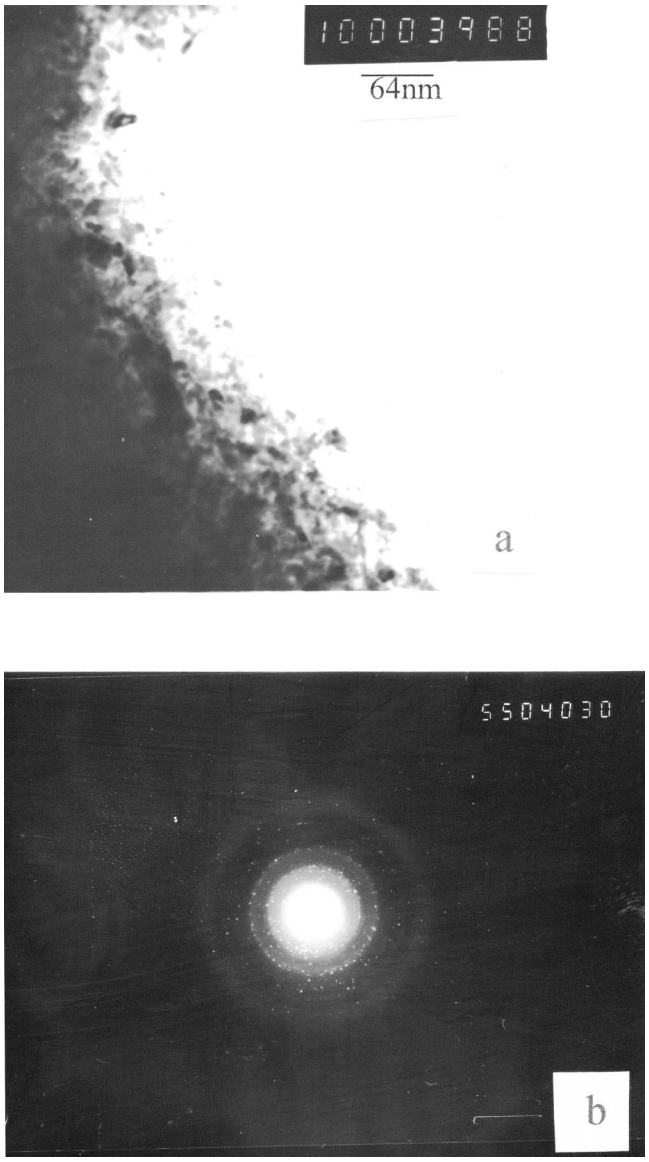

FIG. 2. (a) Transmission electron micrograph of a glass ceramic (Fig. 1) ion exchanged at 583 K for 6 h and subsequently reduced at 573 K for 5 min. (b) Electron diffraction pattern of (a).

shut, and the RH was measured by a Barigo (Germany) Hygrometer made in Germany. By this procedure, it was possible to attain RH values in the range of 25% to 90% within the specimen chamber. The electrical resistance at room temperature was measured for all the samples by a Keithley 617 electrometer.

III. RESULTS AND DISCUSSION

The nucleation and growth temperatures as determined by DTA analysis were 843 and 963 K, respectively.[20] Figure 1 is a scanning electron micrograph of a glass in which the crystalline phases were grown by giving a two-stage heat treatment of 843 K for 6 h followed by 963 K for 15 min. The bright regions in Fig. 1 represent the crystalline phases whereas the dark ones comprise the glass matrix. These are shown by bright and dark arrows, respectively, in Fig. 1. It is seen that crystals of width ~6 μm and length ~40 μm are

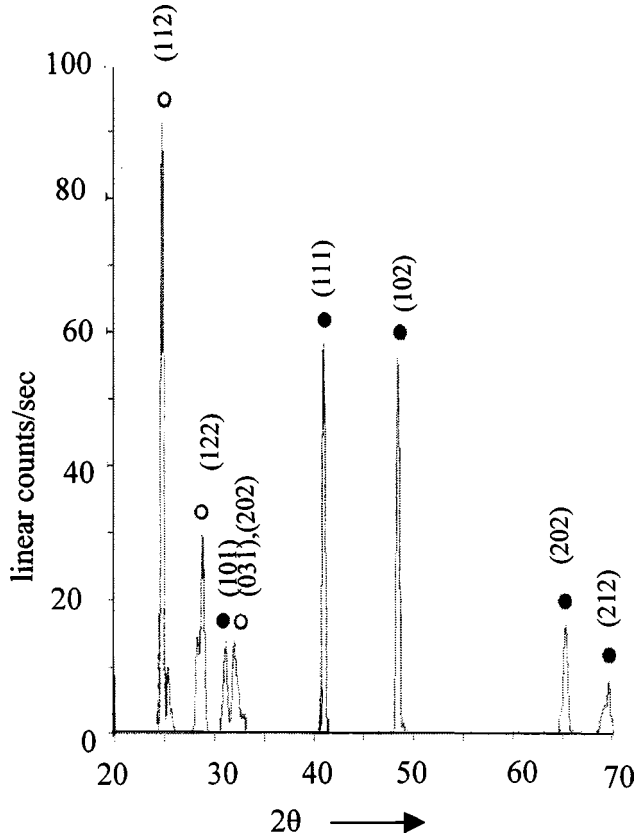

FIG. 3. X-ray diffractogram of the glass ceramic shown in Fig. 1: ○; $Na_2B_4O_7$ and ● $BaTiO_3$.

present within the glass matrix. Figure 2 is the x-ray diffractogram of the glass ceramic. The crystalline phases present were identified as barium titanate and sodium tetraborate, respectively. The corresponding diffraction peaks have been indicated in Fig. 2. The crystal planes giving rise to the different diffraction peaks are indicated by the corresponding Miller indices in Fig. 2. This is typical of all glass–ceramic specimens used here to grow nanoparticles of silver.

Figure 3(a) is the transmission electron micrograph for the glass–ceramic sample shown in Fig. 1 but which was ion exchanged at 583 K for 6 h and, subsequently, reduced at 573 K for 5 min. This is typical of all other glass–ceramic samples after ion exchange and reduction treatment. Figure 3(b) is the electron diffraction pattern obtained from Fig. 3(a). The interplanar spacings d_{hkl} as calculated from the diameters of the diffraction rings are listed in Table I. These values are compared with standard ASTM data for metallic silver. The data confirm that the particles consist of metallic silver.

TABLE I. Comparison of d_{hkl} with standard ASTM data in the case of a specimen heat treated at 843 K for 6 h followed by 963 K for 15 min, and subsequently ion exchanged at 583 K for 6 h and then reduced at 573 K for 5 min.

d_{hkl} (observed) (nm)	d_{hkl} (for silver) (ASTM) (nm)
0.236	0.2359
0.205	0.2044
0.145	0.1445
0.124	0.1231
0.094	0.093 75

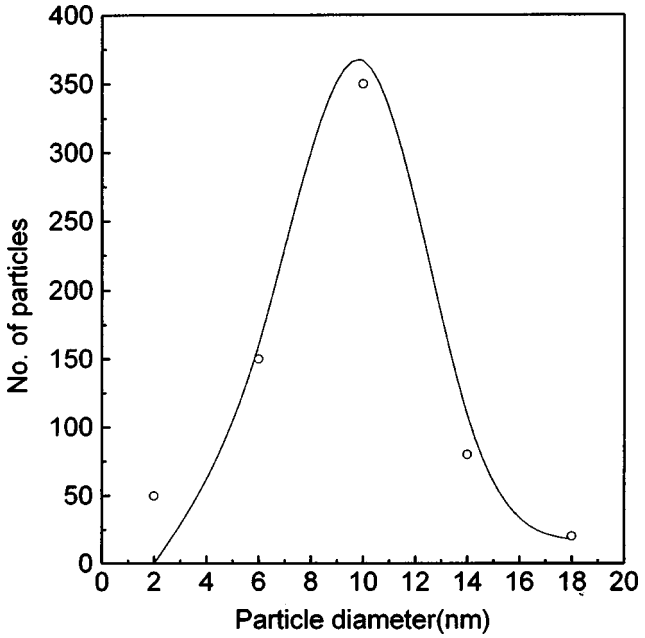

FIG. 4. Histogram of silver particle size obtained from Fig. 3(a).

Figure 4 gives the histogram of silver particle size as obtained from Fig. 3(a). The data were fitted to a log-normal distribution function[18] which is shown by the line in Fig. 4—the points representing the experimental data. The extracted values of median diameter $\bar{x}$ and geometric standard deviation σ are given in Table II along with those of other specimens in the series determined by following an identical procedure as just described. The data in Table II show the marked effect that the heat treatment schedule has on the growth of nanosized metal particles at the glass–crystal interface. This has been ascribed to the effect of crystal morphology on the kinetics of metal phase formation. It has been shown earlier[20] that by changing the heat treatment schedule for precipitating the crystalline phase within the glass, the fractal structure of the crystals can be changed. The metal nanoparticle growth at the glass–crystal interface takes place by a mechanism of heterogeneous nucleation. A fractal dimension ~2.0 indicates a smooth surface of the crystals whereas a value of less than 2.0 implies a rough surface. The latter introduces sites for metal particle growth for which the kinetics of transformation will be much faster than that on a

TABLE II. Summary of heat treatment schedules for crystallization and median diameter $\bar{x}$ and geometric standard deviation σ obtained for different specimens after ion exchange/reduction treatment.

Specimen No.	Heat treatment schedule	$\bar{x}$ (nm)	σ
1	843 K for 2 h+963 K for 10 min	3.4	1.5
2	843 K for 4 h+963 K for 10 min	4.6	1.3
3	843 K for 6 h+963 K for 15 min	10.1	1.3
4	843 K for 2 h+963 K for 20 min	13.2	1.4

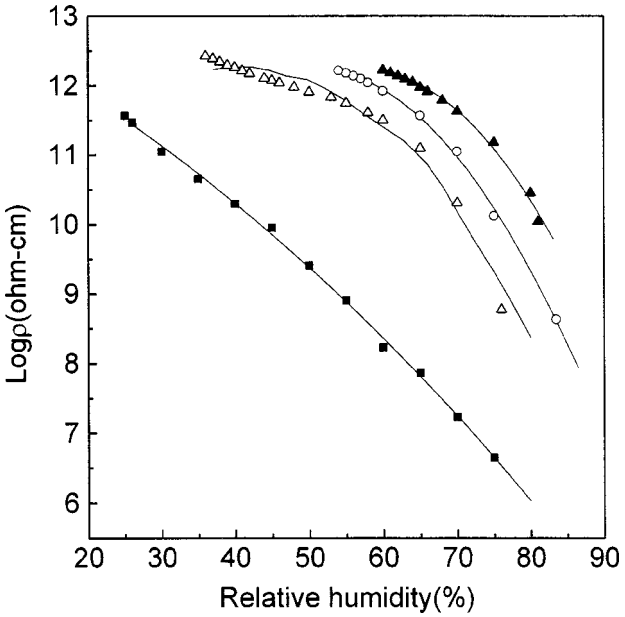

FIG. 5. Resistivity variation as a function of relative humidity for nanocomposites with different silver particle diameter: ▲; 3.4 nm, ○; 4.6 nm, ■; 10.1 nm, and △ 13.2 nm.

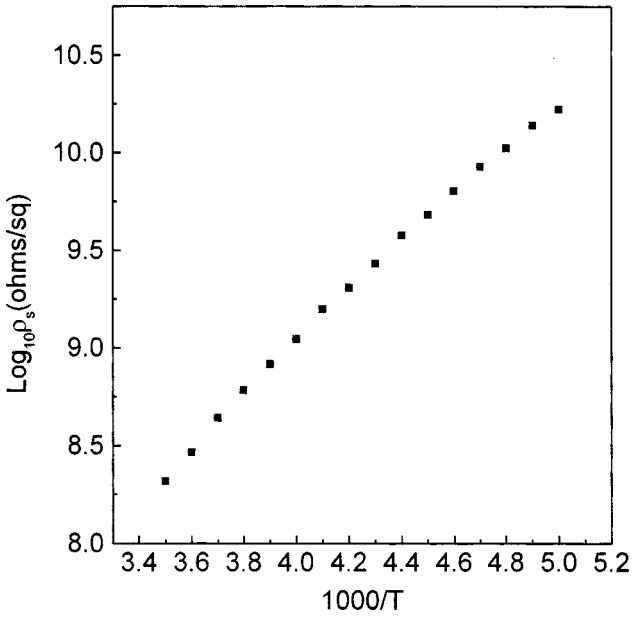

FIG. 6. Log surface resistivity vs inverse temperature for a nanocomposite with silver particle diameter 3.4 nm.

smooth surface. Thus, without altering the ion-exchange temperature/time, as well as reduction treatment schedule, different sizes of nanoparticles of silver could be generated by simply changing the ceramization temperature and time. A detailed discussion has been given elsewhere to explain this effect.[20]

Figure 5 shows the resistivity variation as a function of RH for specimens with different diameters of the silver particles in the nanocomposites. In Fig. 5, the points represent the experimental data and the lines have been fitted by a function given by

$$\rho = \exp\{-(\alpha + \beta_1 \eta + \beta_2 \eta^2)\}, \tag{1}$$

where, ρ is the resistivity, α, β_1, and β_2 are constants, and η is the RH. The fits are found to be satisfactory. In Table III, the values of parameters α, β_1, and β_2 as extracted by this fitting are summarized for the different specimens. The reproducibility and repeatability of the humidity sensing in these materials were checked by the following measurements. Resistivity change as a function of RH was studied for a specimen freshly prepared as well as after a period of 2 months. The two sets of results were in agreement within 1%. Similarly, two specimens were prepared following identical procedure as delineated before. Humidity sensing behavior was then examined for both of them. Here also, the two sets of resistivity values were in agreement within 1%.

TABLE III. Summary of fitting parameters for resistivity change as a function of RH.

Specimen No.	α	β_1	β_2
1	0.4	−0.4	0.004
2	−3.9	−0.3	0.003
3	−13.0	0.05	0.0005
4	−7.9	−0.2	0.002

It is evident that the nanocomposites show a marked change of electrical resistivity of almost five orders of magnitude as the RH is varied from 25% to 85%. It is also to be noted that the sensitivity of the sample is maximum for an optimum value of silver particle diameter viz., 10.1 nm. The surfaces of the silver nanoparticles provide the sites for physisorption of water molecules. As discussed later, we believe that the electrical conduction in the present system arises due to a variable range hopping. The absorption of water molecules increases the density of states responsible for such a hopping conduction mechanism. As the particle size is initially increased, an increase in the total surface area enhances the number of states thereby raising the electrical conductivity. After an optimum diameter of silver particles is reached, however, the volume fraction of the metal phase exerts its influence. The surface-to-volume ratio decreases and, as a consequence, the effective number of sites per unit volume responsible for giving rise to electrical conduction is decreased. This tends to raise the electrical resistivity of the nanocomposites under investigation.

To elucidate the conduction mechanism in the present system, we consider the variation of electrical resistivity as a function of temperature for the nanocomposites. In Fig. 6, we show the $\log \rho_s$ versus inverse temperature ρ_s being the surface resistivity over the range 230 to 333 K for a nanocomposite specimen with silver particle diameter 3.4 nm. It should be noted here that the sample was prepared by subjecting a bulk glass to ceramization treatment followed by ion exchange and reduction reaction, respectively. The electrical measurements were carried out by painting two silver electrodes on the specimen surface with a separation of 1 mm. The measurements were carried out after evacuating the sample chamber to a pressure of 10^{-3} Torr. This procedure was followed in order to obtain a dense enough specimen

with a reasonably low resistance so that meaningful electrical measurements could be carried out to low temperatures. These data are typical of the results obtained for other specimens in the series. We have considered the possibility of an electron tunneling mechanism[22] to be operative in this case. The activation energy ϕ, according to this model, is given by

$$\phi = \frac{1.44}{\varepsilon}\left(\frac{2}{\bar{x}} - \frac{1}{\frac{\bar{x}}{2}+s}\right)\text{eV}, \tag{2}$$

where, ε is the dielectric constant of the dielectric medium containing the metal dispersoids, $\bar{x}$ is the median diameter, and s is the separation between the dispersoids both expressed in nanometers. Taking $\varepsilon \sim 4.0$ (the dielectric constant of the silicate glass) and substituting for s a value of 1.7 nm, in the present case, we calculate a value of $\phi \sim 0.10$ eV. This is much smaller than the activation energy 0.30 eV as estimated from the slope of the line drawn through the data points in Fig. 6. Such differences were noted for other specimens also. We have therefore considered the variable range hopping conduction mechanism[23] for our sample system because this mechanism was found to be appropriate earlier[23,24] in the case of samples having a microstructure similar to that existing in the present case. In this model, the resistivity ρ can be written as

$$\rho = \rho_o \exp\left(\frac{T_o}{T}\right)^{1/4}, \tag{3}$$

where

$$T_o = \frac{8 b_c \chi^3}{pN(E_F)k}, \tag{4}$$

where b_c is a dimensionless quantity having a value of 1.5, p is a proportionality constant which can be taken to be unity, $N(E_F)$ is the density of states near the Fermi level, k is the Boltzmann constant, and χ is the tunneling constant and can be calculated using

$$\chi = \left(\frac{2m\phi}{h^2}\right). \tag{5}$$

In Eq. (4), m is the electron mass, ϕ is the effective barrier height, and h is the Planck constant.

We have plotted the resistivity data given in Fig. 6 as a function of $T^{-1/4}$ in Fig. 7. The straight line fit was obtained using Eq. (2) signifying that the aforementioned model is valid in our case. The value of χ was calculated to be ~ 1 Å^{-1} for silver. From the slope T_o of the straight line in Fig. 7 and substituting the values of different parameters in Eq. (3), we have estimated the value of $N(E_F)$ as 0.8×10^{20} eV^{-1} cc^{-1}. By following the same procedure, the $N(E_F)$ values for specimens 2, 3, and 4 were determined as 1.5×10^{20}, 1.2×10^{20}, and 2.8×10^{20} eV^{-1} cc^{-1}, respectively. Evidently, they are of the same order of magnitude. It should be mentioned here that no physical significance could be attached to T_o values extracted from the slope of the curve shown in Fig. 6. In the theory of Mott[25] and the subsequent experimental verification,[26] the authors had determined the value of the slope and referred to it as simply the gradient. In the case of electrical conductivity data measured for heavily doped germanium,[26] the authors extracted a value of this gradient to be ~ 10.5. According to our representation, this will mean a value of $T_o \sim 1.2\times 10^4$. For the present specimen systems, we have estimated T_o values which are of the order of 10^8. It should be noted that in nanocomposites consisting of iron nanoparticles with an oxide nanolayer around them, a variable range hopping mechanism was also reported to be operative in the temperature range of 110 to 300 K.[24]

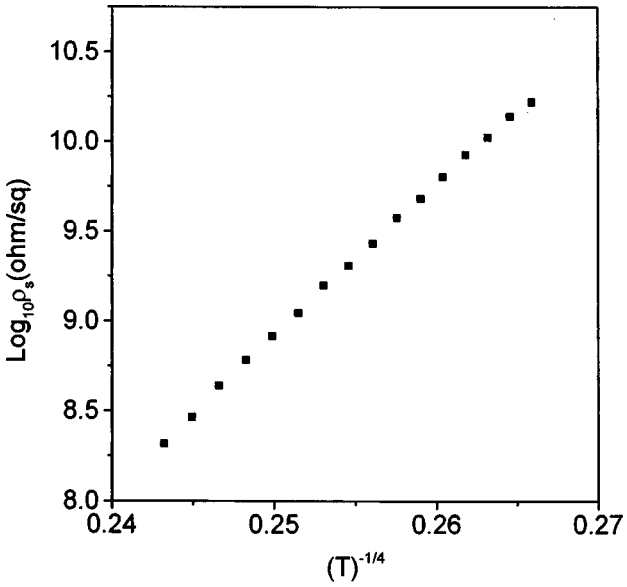

FIG. 7. Log surface resistivity vs $T^{-1/4}$ for a nanocomposite with silver particle diameter 3.4 nm.

It should be noted here that the electrical conductivity in the nanocomposites under humid conditions was checked to be electronic in origin. For this, we show in Fig. 8 the varia-

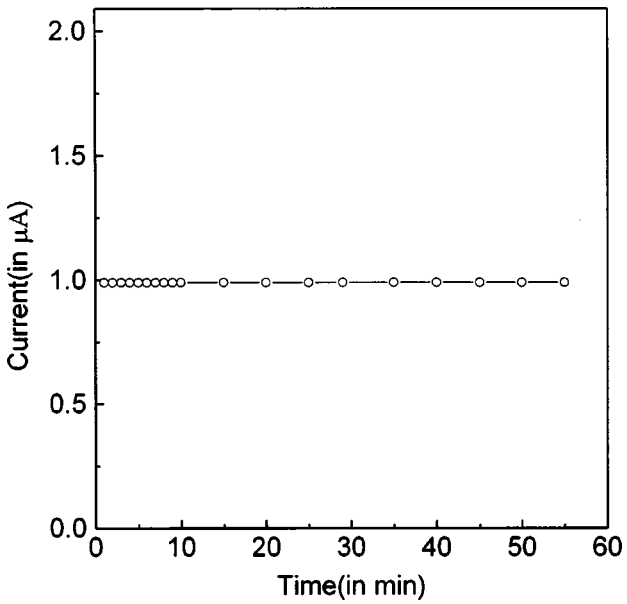

FIG. 8. Variation of current as a function of time for specimen with silver particle diameter 10.1 nm under a RH of 85%. Applied voltage across specimen= 10 V.

tion of current as a function of time with an applied voltage of 10 V for specimen 3 under a RH of 85%. This is typical of all of the other specimens under different humidity conditions. It appears, therefore, that the variable range hopping mechanism is operative also under different RH conditions. The physisorbed water molecules on silver nanoparticles give rise to an increased number of localized states near the Fermi level thereby increasing the value of $N(E_F)$.

In summary, we have synthesized glass–ceramic silver nanocomposites having metal particle diameters in the range of 3.4 to 13.2 nm by controlling the microstructure of the crystalline phase grown within the glass. Electrical resistivity measurements were carried out on cold-pressed samples of nanocomposite powders. Resistivity changes of five orders of magnitude were recorded in the RH range of 25% to 85%. The analysis of resistivity data of the nanocomposite led to the conclusion that a variable range hopping conduction mechanism was operative.

ACKNOWLEDGMENT

One of the authors (B.N.P.) acknowledges the award of a Junior Research Fellowship by C.S.I.R. New Delhi. Another author (D.C.) thanks C.S.I.R. for a research grant.

[1] B. M. Kulwicki, J. Am. Chem. Soc. **74**, 697 (1991).
[2] C. Caliendo, I. Fratoddi, and M. V. Russo, Appl. Phys. Lett. **80**, 4849 (2002).
[3] K. Ogma, T. Tonosaki, and H. Shiigi, J. Electrochem. Soc. **148**, H21 (2001).
[4] M. Tong, G. Dai, Y. Wu, X. He, W. Yan, D. Gao, V. Volkov, and G. Zakharova, J. Mater. Res. **15**, 2653 (2000).
[5] D. Das, M. Pal, E. Di Bartolomeo, E. Traversa, and D. Chakravorty, J. Appl. Phys. **88**, 6856 (2000).
[6] C. A. Grimes, D. Kouzoudis, E. C. Dickey, D. Qian, M. A. Anderson, R. Shahidain, M. Lindsey, and L. Green, J. Appl. Phys. **87**, 5341 (2000).
[7] G. H. Cross, Y. Ren, and N. J. Freeman, J. Appl. Phys. **86**, 6483 (1999).
[8] M. J. Hogan, A. W. Brinkman, and T. Hashemi, Appl. Phys. Lett. **72**, 3077 (1998).
[9] M. Matsuguchi, Y. Sadaoka, Y. Sakai, T. Kuroiwa, and A. Ito, J. Electrochem. Soc. **138**, 1862 (1991).
[10] Y. Sakai, Sens. Actuators B **13**, 82 (1993).
[11] J. Arndt, in *Sensors: A Comprehensive Survey*, edited by W. Gopel, J. Hesse, and J. N. Zemel (VCH, Weinheim, 1989), Vol. 1, pp. 247–278.
[12] J. G. Fagan and V. R. W. Amarakoon, Am. Ceram. Soc. Bull. **72**, 119 (1993).
[13] J. H. Anderson and G. A. Parks, J. Phys. Chem. **72**, 3362 (1968).
[14] N. Yamazoe, J. Fuchigami, M. Kishikawa, and T. Seiyama, Surf. Sci. **86**, 335 (1979).
[15] S. Banerjee, S. Banerjee, A. Datta, and D. Chakravorty, Europhys. Lett. **46**, 346 (1999).
[16] S. Roy and D. Chakravorty, J. Phys.: Condens. Matter **6**, 8599 (1994).
[17] M. Mukherjee, A. Datta, and D. Chakravorty, J. Mater. Res. **12**, 2507 (1997).
[18] B. Roy and D. Chakravorty, J. Phys.: Condens. Matter **2**, 9323 (1990).
[19] T. K. Kundu and D. Chakravorty, J. Phys. Soc. Jpn. **65**, 3401 (1996).
[20] T. K. Kundu, S. Banerjee, and D. Chakravorty, Jap. Jpn. J. Appl. Phys. (to be published).
[21] B. Roy, S. Roy, and D. Chakravorty, J. Mater. Res. **9**, 2677 (1994).
[22] P. A. Tick and F. P. Fehlner, J. Appl. Phys. **43**, 362 (1972).
[23] P. Sheng, in *Nanophase Materials*, edited by G. C. Hadjipanayis and R. W. Siegel (Kluwer, Dordrecht, 1994), p. 381.
[24] S. Banerjee, A. K. Ghosh, and D. Chakravorty, J. Appl. Phys. **86**, 6835 (1999).
[25] N. F. Mott, Philos. Mag. **26**, 1015 (1972).
[26] F. R. Allen and C. J. Adkins, Philos. Mag. **26**, 1027 (1972).